Low-Temperature Heat Capacities and Ferromagnetic Phase Transition of the Organic Free Radical Ferromagnet, 4-(4-Chlorobenzylideneamino)-2,2,6,6-tetramethylpiperidin-1-oxyl (CATMP)#

Yuji Miyazaki, Tetsuya Matsumoto, Takayuki Ishida,† Takashi Nogami,† and Michio Sorai*

Research Center for Molecular Thermodynamics, Graduate School of Science, Osaka University, Toyonaka, Osaka 560-0043

†Department of Applied Physics and Chemistry, The University of Electro-Communications, Chofugaoka, Chofu, Tokyo 182-8585

(Received September 16, 1999)

Heat capacities of the organic free radical ferromagnet, 4-(4-chlorobenzylideneamino)-2,2,6,6-tetramethylpiperidin-1-oxyl (CATMP) have been measured in the temperature range between 0.1 and 311 K. A ferromagnetic phase transition was observed at 0.28 K and a heat capacity hump was found above the transition temperature. This hump is due to the short-range order characteristic of low-dimensional magnetic spin systems. The enthalpy and entropy gains due to the ferromagnetic phase transition were estimated to be 4.06 J mol^{-1} and 5.71 J K^{-1} mol^{-1}, respectively. This entropy agrees well with the theoretical value $R\ln 2$ (= 5.76 J K^{-1} mol^{-1}) expected for the magnetic entropy of a spin system with the spin quantum number $S = 1/2$, where R is the gas constant. The heat capacity hump above the transition temperature is well accounted for in terms of the $S = 1/2$ two-dimensional ferromagnetic Heisenberg model of square lattice with the intralayer exchange interaction $J/k_B = 0.42$ K, where the spin Hamiltonian $\boldsymbol{H} = -2J\boldsymbol{S}_i\cdot\boldsymbol{S}_j$ is adopted and k_B stands for the Boltzmann constant. The analysis of the magnetic heat capacities below the transition temperature on the basis of the spin wave theory clarified that the magnetic system settles down in three-dimensional ferromagnetic order below the transition temperature with the interlayer exchange interaction $J'/k_B = 0.024$ K.

Since the discovery of ferromagnetism in the β-phase of p-nitrophenylnitronyl nitroxide (p-NPNN),[1—5] synthesis of purely organic ferromagnets has been developed extensively. Nearly twenty kinds of organic free radical ferromagnets have so far been synthesized and investigated experimentally and theoretically.[1—27] It has been reported recently that the β-phase of the dithiadiazolyl radical p-NC·C_6F_4·CNSSN orders as a weak ferromagnet below $T_N = 35.5$ K,[25—27] which is the highest transition temperature ever reported.

The present organic free radical 4-(4-chlorobenzylideneamino)-2,2,6,6-tetramethylpiperidin-1-oxyl (CATMP, Fig. 1) is one of the 2,2,6,6-tetramethylpiperidin-1-oxyl (TEMPO) derivatives, which show a variety of magnetism types depending on the type of substituent group.[14—24,28—33] The X-ray crystallographic analysis and computational approach[17,19] predicted that the CATMP free radical crystal possesses a two-dimensional ferromagnetic network. The magnetic measurement[17] indicated that the CATMP crystal gives rise to a feromagnetic phase transition at ca. 0.4 K. A typical ferromagnetic M(magnetization)–H(magnetic field) curve with a narrow hysteresis loop is observed below the transition temperature. The zero-field muon spin rotation and relaxation (μSR) experiment[21] revealed that the CATMP crystal has a three-dimensional Heisenberg type ordering below the Curie temperature $T_C = 0.28$ K, which is somewhat lower than T_C = ca. 0.4 K previously reported.[17]

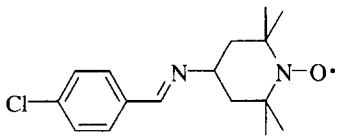

Fig. 1. Molecular structure of CATMP.

Heat capacity measurement for magnetic materials is one of the most effective tools to get information about precise magnetic phase transition temperature, spin–spin interaction, magnetic dimensionality, and type of magnetism. Our research group has so far investigated some TEMPO radical derivatives by means of adiabatic calorimetry,[28,29,32] and revealed some important aspects. The objective of the present research is to measure accurately the heat capacity of the CATMP crystal and to elucidate its magnetic properties in detail.

Experimental

The preparation of CATMP was carried out according to a method described elsewhere.[14,15] Two types of adiabatic calorimeters were employed: one is a very-low-temperature adiabatic calorimeter workable with a ^{3}He/^{4}He dilution refrigerator[34] (dilution calorimeter for short) from 0.1 to 19 K and the other is a low-tempera-

Contribution No. 10 from the Research Center for Molecular Thermodynamics.

ture adiabatic calorimeter for small samples[35] (microcalorimeter for short) from 10 to 311 K. For the dilution calorimeter, 0.94629 g of the sample was formed into a disc (2 cm diameter and ca. 2 mm thickness) and loaded into a gold-plated copper cell without any heat exchange media. On the other hand, for the microcalorimeter, 0.53432 g of the sample was loaded in a 1.2 cm^3 gold-plated copper cell together with helium gas at ambient pressure to facilitate thermal equilibration. Buoyancy correction for the sample weights was made by assuming a density of 1.217 $g\,cm^{-3}$.[17,19]

Results and Discussion

The molar heat capacities at constant pressure, C_p, of the CATMP free radical crystal are tabulated in Table 1 and plotted in Fig. 2. A heat capacity peak due to a phase transition was observed at 0.28 K, which is slightly lower than T_C = ca. 0.4 K determined by the magnetic measurement[17] but in good agreement with T_C = 0.28 K obtained by the μSR study.[21] Therefore this phase transition can be regarded as the ferromagnetic phase transition. Above the transition temperature, a heat capacity hump was also observed. This thermal anomaly is attributed to the short-range ordering effect of spins characteristic of low-dimensional magnets.

In order to evaluate the excess (or magnetic) heat capacities, the lattice heat capacities were estimated as follows. The lattice heat capacities C_p(lattice) at very low temperatures T are often approximated by the temperature polynomial with odd powers:

$$C_p(\text{lattice}) = \sum_{i=1}^{n} c_i T^{2i+1}, \quad (1)$$

which corresponds to a series expansion of the Debye function with respect to T. The heat capacity anomaly arising from the short-range order of a spin system is known to be proportional to T^{-2} at high enough temperatures.[36] Hence the entire heat capacity involving contributions of both the lattice vibration and the short-range order is given by the next equation

$$C_p = \sum_{i=1}^{n} c_i T^{2i+1} + c_{n+1} T^{-2}. \quad (2)$$

In the present case, we could fit well the heat capacity data between 2 and 10 K to Eq. 2 with $n = 3$ and the respective coefficients were determined to be $c_1 = 7.233\times10^{-3}\,J\,K^{-4}\,mol^{-1}$, $c_2 = -3.889\times10^{-5}\,J\,K^{-6}\,mol^{-1}$, $c_3 = 2.852\times10^{-7}\,J\,K^{-8}\,mol^{-1}$, and $c_4 = 2.628\,J\,K\,mol^{-1}$. The derived lattice heat capacity curve is drawn in Fig. 2(a) by a solid curve.

The magnetic heat capacities of the sample were evaluated by subtracting the lattice heat capacities from the total heat capacities. Figure 3 indicates the magnetic heat capacities ΔC_p of the CATMP crystal. The enthalpy and entropy

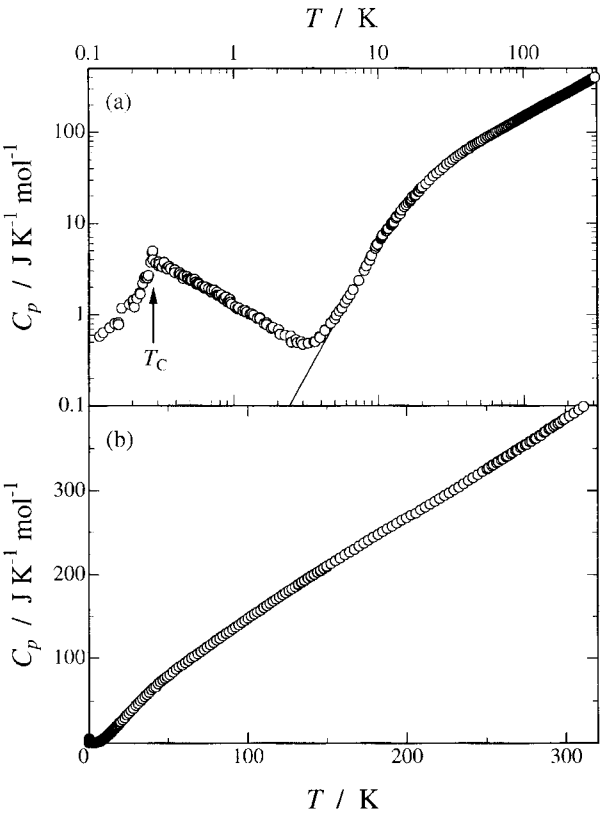

Fig. 2. Molar heat capacities of CATMP free radical crystal on (a) logarithmic and (b) normal scales. Solid curve indicates calculated lattice heat capacities.

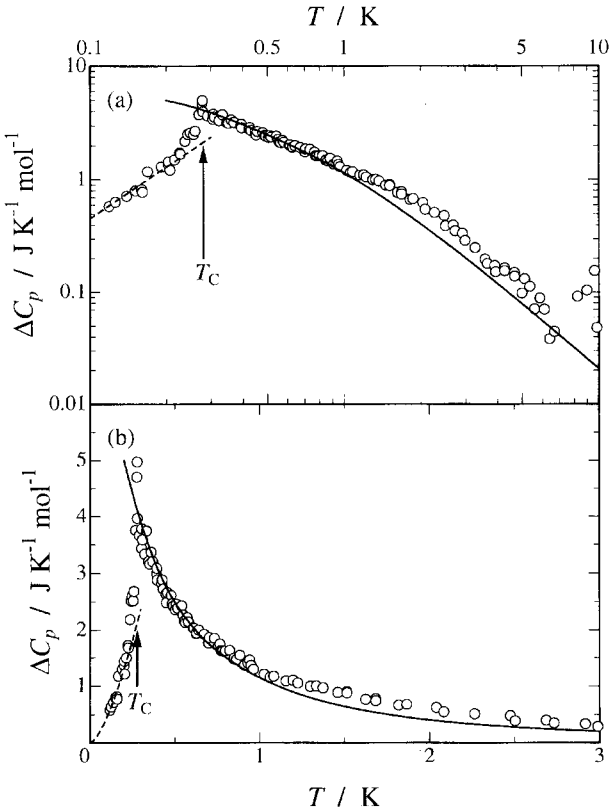

Fig. 3. Magnetic heat capacities of CATMP free radical crystal on (a) logarithmic and (b) normal scales. Solid curves indicate the heat capacities calculated from the high-temperature series expansion for the $S = 1/2$ two-dimensional ferromagnetic Heisenberg model of square lattice with $J/k_B = 0.42$ K. Broken curves show the heat capacities derived from the spin wave theory for three-dimensional ferromagnets.

Table 1. Molar Heat Capacities of CATMP (M = 293.82 g mol^{-1})
Data in series 1—6 and series 7—10 were collected by use of different adiabatic calorimeters.

T/K	C_p/J K^{-1} mol^{-1}	T/K	C_p/J K^{-1} mol^{-1}	T/K	C_p/J K^{-1} mol^{-1}	T/K	C_p/J K^{-1} mol^{-1}	T/K	C_p/J K^{-1} mol^{-1}	T/K	C_p/J K^{-1} mol^{-1}
series 1		0.216	1.499	12.33	9.517	179.07	244.1	10.71	7.217	104.12	153.0
0.204	1.367	0.227	1.685	13.29	11.43	182.05	247.2	11.59	8.639	106.10	155.4
0.256	2.517	0.237	2.191	14.26	12.76	185.02	250.9	12.49	10.22	108.08	157.6
0.277	4.708	0.249	2.600	17.22	19.65	188.00	254.2	13.45	11.93	110.05	160.6
0.310	3.588	0.260	2.687	18.23	20.66	190.97	257.1	14.49	13.87	112.03	163.2
0.352	3.160	0.269	3.755	19.24	22.61	193.95	260.8	15.57	15.98	114.02	165.7
0.396	2.883	0.279	3.969			196.92	264.4	16.69	18.20	116.00	168.4
0.448	2.642	0.291	3.660	series 6		199.90	267.0	17.83	20.16	117.98	170.8
0.504	2.365	0.305	3.433	0.912	1.378	202.87	270.6	18.98	22.69	119.96	173.3
0.564	2.134	0.323	3.334	1.026	1.217	205.85	272.7	20.14	25.13	121.94	176.0
0.629	1.951	0.346	3.208	1.155	1.105	208.83	277.1	21.36	27.25	123.92	178.3
0.699	1.784	0.370	3.206	1.298	1.012	211.80	280.4	22.64	30.05	125.90	180.9
0.774	1.640	0.395	3.088	1.461	0.912	214.78	283.8	23.96	33.21	127.88	183.1
0.851	1.504	0.423	2.822	1.626	0.802	217.76	287.2	25.31	35.56	129.86	185.6
0.932	1.412	0.451	2.490	1.821	0.712	220.74	290.8	26.69	38.43	131.85	188.2
		0.479	2.614	2.041	0.687	223.71	294.5	28.13	41.01	133.83	190.6
series 2		0.511	2.460	2.266	0.596	226.69	297.6	29.61	44.71	135.82	193.0
0.432	2.730	0.541	2.431	2.476	0.588	229.67	301.2	31.11	47.03	137.80	195.9
0.492	2.427	0.574	2.226	2.686	0.533	232.65	304.5	32.57	49.99	139.79	197.9
0.557	2.164	0.609	2.042	2.918	0.509	235.63	308.4	33.96	52.50	141.78	200.2
0.628	1.941	0.642	2.003	3.650	0.509	238.62	312.3	35.35	55.15	143.76	202.7
0.703	1.771	0.674	1.929	3.944	0.563	241.60	315.8	36.75	57.54	145.75	204.4
0.782	1.625	0.705	1.871	4.275	0.672	244.58	319.2	38.14	60.02	147.74	207.4
0.865	1.475	0.735	1.859	4.677	0.806	247.56	322.9	39.54	62.81	149.72	209.3
0.951	1.373	0.767	1.760	5.000	0.903	250.55	326.3	40.94	65.01		
1.062	1.165	0.799	1.634	5.365	1.093	253.53	329.9	42.35	66.27	series 10	
1.197	1.116	0.825	1.643	5.872	1.350	256.51	333.6	43.77	69.87	251.52	327.3
1.334	1.022	0.884	1.554	6.410	1.649	259.50	336.9	45.19	72.22	254.51	331.1
1.514	0.930	0.942	1.470	8.260	3.420	262.48	340.4	46.61	74.36	257.50	334.4
1.685	0.815			8.991	4.429	265.46	343.7	48.05	76.28	260.49	337.8
		series 5		9.834	5.887	268.45	347.7	49.48	78.35	263.49	341.3
series 3		0.849	1.490	10.75	7.378	271.43	351.2	51.16	80.43	266.48	345.2
0.126	0.638	0.963	1.304	11.75	8.726	274.41	354.5	53.07	83.94	269.47	348.4
0.160	0.819	1.083	1.183	12.83	10.23	277.40	358.0	54.99	86.84	272.47	352.3
0.207	1.215	1.226	1.067	13.99	12.77	280.38	361.5	56.92	89.90	275.46	355.1
0.226	1.730	1.373	0.989	16.61	17.45	283.36	364.9	58.85	91.89	278.45	358.7
0.243	2.516	1.515	0.908	18.12	20.18	286.34	369.0	60.79	94.65	281.45	362.1
0.278	4.977	1.686	0.779			289.32	372.9	62.74	97.22	284.44	365.4
0.306	3.783	1.867	0.727	series 7		292.30	375.7	64.69	100.3	287.43	370.1
0.333	3.744	2.085	0.612	131.98	188.7	295.27	379.2	66.64	102.4	290.42	373.9
0.360	3.366	2.505	0.502	133.98	191.2	298.25	383.1	68.60	105.2	293.41	377.4
0.393	2.996	2.734	0.496	135.96	193.5			70.57	107.7	296.40	380.6
0.427	2.887	2.991	0.475	137.94	195.8	series 8		72.53	110.4	299.39	384.7
0.457	2.666	3.270	0.489	139.92	198.4	9.623	5.570	74.50	113.3	302.39	387.8
0.487	2.471	3.578	0.508	141.91	200.6	10.52	6.967	76.47	115.8	305.38	391.1
0.517	2.396	3.910	0.573	143.89	202.8	11.44	8.309	78.44	118.6	308.37	395.1
0.549	2.272	4.273	0.681	145.88	205.3	12.35	9.860	80.42	121.6	311.36	398.8
0.581	2.151	4.674	0.816	147.86	207.7	13.28	11.55	82.39	123.8		
0.613	2.038	5.113	0.988	149.84	210.0	14.21	13.37	84.37	126.7		
		5.595	1.173	152.32	213.0	15.13	15.22	86.35	129.4		
series 4		6.120	1.486	155.29	216.4	16.07	16.91	88.34	131.8		
0.119	0.583	6.696	1.865	158.26	219.9	16.99	18.60	90.32	134.5		
0.140	0.718	7.326	2.354	161.23	223.5	17.93	20.51	92.29	137.2		
0.151	0.801	8.012	3.038	164.20	226.9	18.81	22.47	94.26	139.8		
0.161	0.779	8.756	3.933	167.18	229.9	19.65	24.35	96.24	142.6		
0.169	1.175	9.561	5.303	170.15	233.8			98.20	145.1		
0.191	1.299	10.44	6.766	173.12	237.1	series 9		100.17	147.8		
0.204	1.441	11.37	8.211	176.09	240.6	9.886	5.867	102.15	150.4		

acquisitions due to the ferromagnetic phase transition were calculated as follows. The enthalpy and entropy gains from the lowest temperature 0.1 K studied here to 7.3 K were calculated by directly integrating the ΔC_p values with respect to T and ln T, respectively. Those from 0 to 0.1 K were evaluated on the basis of the spin wave theory, which is described below. Those from 7.3 K to infinite temperature were estimated by use of the T^{-2} term of Eq. 2. The magnetic enthalpy and entropy thus determined amounted to 4.06 J mol^{-1} and 5.71 J K^{-1} mol^{-1}, respectively. This magnetic entropy is in excellent agreement with the value Rln 2 (= 5.76 J K^{-1} mol^{-1}) expected for the magnetic system consisting of spins with spin quantum number $S = 1/2$, where R is the gas constant. This fact means that the present specimen indeed consists of pure radicals in which each molecule has a single unpaired electron and that the observed heat capacity anomaly arises from the reorientational mechanism of $S = 1/2$ spins.

In order to examine the nature of the ferromagnetic phase transition found in the CATMP crystal in detail, we analyzed the magnetic heat capacities below and above the transition temperature T_C. At first, we tried to fit several $S = 1/2$ Heisenberg models to the heat capacity hump above T_C. As shown in Fig. 3 by solid curves, the best fit was obtained for the $S = 1/2$ two-dimensional ferromagnetic Heisenberg model[37] of square lattice with the intralayer exchange interaction $J/k_B = 0.42$ K, where the spin Hamiltonian $\boldsymbol{H} = -2J\boldsymbol{S}_i \cdot \boldsymbol{S}_j$ is adopted and k_B denotes the Boltzmann constant. Here we used the Padé approximation in fitting the magnetic heat capacities to the model. This result is consistent with the two-dimensional ferromagnetic network structure predicted from the X-ray crystallographic analysis and computational approach,[17,19] but this two-dimensional network structure is not regarded as a square lattice. There may exist two different intralayer exchange interactions J_1 and J_2, as seen from the crystal structure of CATMP.[17,19] However, since the heat capacity anomaly above T_C is well explained by the $S = 1/2$ two-dimensional ferromagnetic Heisenberg model of square lattice, it is very likely that the CATMP crystal possesses a two-dimensional magnetic structure with $J_1 \approx J_2$.

Next, we discuss the low-temperature behavior of the magnetic heat capacities. Spin wave theory is a good approximation to describe the low-temperature properties of magnetic substances. The low-temperature heat capacity due to the spin wave (magnon) excitation C_{SW} can be expressed by the formula[38]

$$C_{SW} \propto T^{d/n}, \tag{3}$$

where d stands for the dimensionality of magnetic lattice and n is defined as the exponent in the dispersion relation: $n = 1$ for antiferromagnets and $n = 2$ for ferromagnets. We fitted the next equation to the magnetic heat capacities between 0.12 and 0.23 K:

$$\Delta C_p = aT^{\alpha}. \tag{4}$$

The parameter value was determined to be $\alpha = 1.68$. Since this value is close to 3/2, we can conclude that the CATMP crystal is in a three-dimensional ferromagnetic state below the transition temperature. Hence we fitted again Eq. 4 with $\alpha = 3/2$ to the magnetic heat capacities in the same temperature range, which yields $a = 14.44$ J K$^{-5/2}$ mol^{-1}. The spin wave heat capacity thus obtained is shown in Fig. 3 by broken curves. This result derived from the spin wave analysis coincides with the three-dimensional ferromagnetism below T_C suggested by the μSR experiment.[21]

More exactly, C_{SW} in a three-dimensional ferromagnet possessing non-equivalent spin–spin interaction paths is expressed as follows:[32]

$$C_{SW} = \frac{5R\zeta(5/2)\Gamma(5/2)}{16\pi^2 S^{3/2}} \left(\frac{k_B^3}{2J_1J_2J_3}\right)^{1/2} T^{3/2}, \tag{5}$$

where J_1, J_2, and J_3 are the positive exchange interaction parameters for three directions, ζ is Riemann's zeta function, Γ is Euler's gamma function, and S denotes the spin quantum number. In the present case, $J_1 = J_2 = J$($= 0.42k_B$ K), $J_3 = J'$, which is an interlayer exchange interaction, and $S = 1/2$. Comparison between Eqs. 4 and 5 brings about $J'/k_B = 0.024$ K.

Nogami et al. have discussed the mechanism of the intrasheet intermolecular ferromagnetic interactions between the N–O sites in some TEMPO derivative radical crystals having two-dimensional sheet structures.[19] Four two-dimensional ferromagnetic TEMPO derivative radical crystals Ar–CH=N–TEMPO (Ar = phenyl, 4-(methylthio)phenyl, 4-chlorophenyl, and 4-biphenylyl) have about 6 Å of the distances between the N–O sites in a intrasheet.[14,15,17–19] Since direct through-space exchange[39,40] and dipole-dipole[41] interactions are very weak, the magnetic interactions arising from such long distances cannot explain $T_C = 0.3$—0.4 K.[14,15,17,18] Nogami et al. proposed a spin polarization mechanism through intervening aliphatic groups as a possible mechanism of the intrasheet ferromagnetic interaction.[17,19] Moreover they have carried out ab initio and semiempirical calculations of the dimer of the phenyl–CH=N–TEMPO compound along the c axis to verify this mechanism.[19,23] The effective exchange integrals calculated by the approximately spin projected UHF (APUHF) method by the use of the 4-31 G basis set and INDO parametrization were evaluated to be 0.236 and 0.014 K, respectively, the larger of which is the same order of magnitude as the average intralayer exchange interaction $J/k_B = 0.42$ K estimated in this work. This supports the validity of the spin-alternation mechanism.

The mechanism for the intersheet ferromagnetic interactions between the ferromagnetic sheets separated by 11—14 Å in the above Ar–CH=N–TEMPO compounds has not yet been understood clearly. Dipolar interactions between the ferromagnetic sheets suggested by Drillon et al.[42] might be a plausible mechanism. In the present study, we could estimate the interlayer ferromagnetic exchange interaction ($J'/k_B = 0.024$ K). This value would provide a good clue to develop adequate models for the interlayer ferromagnetic interaction.

This work was partially supported by a Grant-in-Aid for Scientific Research on Priority Areas "Metal-Assembled

Complexes" (Area No. 401/11136226) from the Ministry of Education, Science, Sports and Culture.

References

1 M. Kinoshita, P. Turek, M. Tamura, K. Nozawa, D. Shiomi, Y. Nakazawa, M. Ishikawa, M. Takahashi, K. Awaga, T. Inabe, and Y. Maruyama, *Chem. Lett.*, **1991**, 1225.

2 M. Takahashi, P. Turek, Y. Nakazawa, M. Tamura, K. Nozawa, D. Shiomi, M. Ishikawa, and M. Kinoshita, *Phys. Rev. Lett.*, **67**, 746 (1991).

3 M. Tamura, Y. Nakazawa, D. Shiomi, K. Nozawa, Y. Hosokoshi, M. Ishikawa, M. Takahashi, and M. Kinoshita, *Chem. Phys. Lett.*, **186**, 401 (1991).

4 Y. Nakazawa, M. Tamura, N. Shirakawa, D. Shiomi, M. Takahashi, M. Kinoshita, and M. Ishikawa, *Phys. Rev. B*, **46**, 8906 (1992).

5 M. Takahashi, M. Kinoshita, and M. Ishikawa, *J. Phys. Soc. Jpn.*, **61**, 3745 (1992).

6 R. Chiarelli, A. Rassat, and P. Pey, *J. Chem. Soc., Chem. Commun.*, **1992**, 1081.

7 R. Chiarelli, M. A. Novak, A. Rassat, and J. L. Tholence, *Nature*, **363**, 147 (1993).

8 T. Sugawara, M. M. Matsushita, A. Izuoka, N. Wada, N. Takeda, and M. Ishikawa, *J. Chem. Soc., Chem. Commun.*, **1994**, 1723.

9 J. Cirujeda, M. Mas, E. Molins, F. L. Panthou, J. Laugier, J. G. Park, C. Paulsen, P. Rey, C. Rovira, and J. Veciana, *J. Chem. Soc., Chem. Commun.*, **1995**, 709.

10 A. Caneschi, F. Ferraro, D. Gatteschi, A. Lirzin, M. A. Novak, E. Rentschler, and R. Sessoli, *Adv. Mater.*, **7**, 476 (1995).

11 K. Mukai, K. Konishi, K. Nedachi, and K. Takeda, *J. Magn. Magn. Mater.*, **140-144**, 1449 (1995).

12 K. Takeda, T. Hamano, T. Kawae, M. Hidaka, M. Takahashi, S. Kawasaki, and K. Mukai, *J. Phys. Soc. Jpn.*, **64**, 2343 (1995).

13 T. Sugimoto, M. Tsuji, T. Suga, N. Hosoito, M. Ishikawa, and N. Takeda, *Mol. Cryst. Liq. Cryst.*, **272**, 183 (1995).

14 T. Nogami, K. Tomioka, T. Ishida, H. Yoshikawa, M. Yasui, F. Iwasaki, H. Iwamura, N. Takeda, and M. Ishikawa, *Chem. Lett.*, **1994**, 29.

15 T. Ishida, H. Tsuboi, T. Nogami, H. Yoshikawa, M. Yasui, F. Iwasaki, H. Iwamura, N. Takeda, and M. Ishikawa, *Chem. Lett.*, **1994**, 919.

16 T. Nogami, T. Ishida, H. Yoshikawa, M. Yasui, F. Iwasaki, H. Iwamura, N. Takeda, and M. Ishikawa, *Synth. Met.*, **71**, 1813 (1995).

17 T. Nogami, T. Ishida, H. Tsuboi, H. Yoshikawa, H. Yamamoto, M. Yasui, F. Iwasaki, H. Iwamura, N. Takeda, and M. Ishikawa, *Chem. Lett.*, **1995**, 635.

18 T. Nogami, T. Ishida, M. Yasui, F. Iwasaki, H. Iwamura, N. Takeda, and M. Ishikawa, *Mol. Cryst. Liq. Cryst.*, **279**, 97 (1996).

19 T. Nogami, T. Ishida, M. Yasui, F. Iwasaki, N. Takeda, M. Ishikawa, T. Kawakami, and K. Yamaguchi, *Bull. Chem. Soc. Jpn.*, **69**, 1841 (1996).

20 K. Togashi, R. Imachi, K. Tomioka, H. Tsuboi, T. Ishida, T. Nogami, N. Takeda, and M. Ishikawa, *Bull. Chem. Soc. Jpn.*, **69**, 2821 (1996).

21 R. Imachi, T. Ishida, T. Nogami, S. Ohira, K. Nishiyama, and K. Nagamine, *Chem. Lett.*, **1997**, 233.

22 T. Nogami, R. Imachi, T. Ishida, N. Takeda, and M. Ishikawa, *Mol. Cryst. Liq. Cryst.*, **305**, 211 (1997).

23 T. Kawakami, A. Oda, S. Takeda, W. Mori, T. Ishida, M. Yasui, F. Iwasaki, T. Nogami, and K. Yamaguchi, *Mol. Cryst. Liq. Cryst.*, **306**, 141 (1997).

24 G. Maruta, S. Takeda, T. Kawakami, W. Mori, R. Imachi, T. Ishida, T. Nogami, and K. Yamaguchi, *Mol. Cryst. Liq. Cryst.*, **306**, 307 (1997).

25 A. J. Banister, N. Bricklebank, I. Lavender, J. M. Rawson, C. I. Gregory, B. K. Tanner, W. Clegg, M. R. S. Elsegood, and F. Palacio, *Angew. Chem., Int. Ed. Engl.*, **35**, 2533 (1996).

26 F. Palacio, M. Castro, G. Antorrena, R. Burriel, C. Ritter, N. Bricklebank, J. Rawson, and J. N. B. Smith, *Mol. Cryst. Liq. Cryst.*, **306**, 293 (1997).

27 F. Palacio, G. Antorrena, M. Castro, R. Burriel, J. Rawson, J. N. B. Smith, N. Bricklebank, J. Novoa, and C. Ritter, *Phys. Rev. Lett.*, **79**, 2336 (1997).

28 H. Sugimoto, H. Aota, A. Harada, Y. Morishima, M. Kamachi, W. Mori, M. Kishita, N. Ohmae, M. Nakano, and M. Sorai, *Chem. Lett.*, **1991**, 2095.

29 M. Kamachi, H. Sugimoto, A. Kajiwara, A. Harada, Y. Morishima, W. Mori, N. Ohmae, M. Nakano, M. Sorai, T. Kobayashi, and K. Amaya, *Mol. Cryst. Liq. Cryst.*, **232**, 53 (1993).

30 T. Kobayashi, M. Takiguchi, K. Amaya, H. Sugimoto, A. Kajiwara, A. Harada, and M. Kamachi, *J. Phys. Soc. Jpn.*, **62**, 3239 (1993).

31 A. Kajiwara, H. Sugimoto, and M. Kamachi, *Bull. Chem. Soc. Jpn.*, **67**, 2373 (1994).

32 N. Ohmae, A. Kajiwara, Y. Miyazaki, M. Kamachi, and M. Sorai, *Thermochim. Acta*, **267**, 435 (1995).

33 A. Kajiwara, W. Mori, M. Sorai, K. Yamaguchi, and M. Kamachi, *Mol. Cryst. Liq. Cryst.*, **272**, 67 (1995).

34 S. Murakawa, T. Wakamatsu, M. Nakano, M. Sorai, and H. Suga, *J. Chem. Thermodyn.*, **19**, 1275 (1987).

35 Y. Kume, Y. Miyazaki, T. Matsuo, and H. Suga, *J. Phys. Chem. Solids*, **53**, 1297 (1992).

36 H. M. J. Blöte, *Physica, B*, **79B**, 427 (1975).

37 G. A. Baker, Jr., H. E. Gilbert, J. Eve, and G. S. Rushbrooke, *Phys. Lett.*, **25A**, 207 (1967).

38 L. J. de Jongh and A. R. Miedema, *Adv. Phys.*, **23**, 1 (1974).

39 T. Kawakami, S. Yamanaka, W. Mori, K. Yamaguchi, A. Kajiwara, and M. Kamachi, *Chem. Phys. Lett.*, **235**, 414 (1995).

40 T. Kawakami, S. Yamanaka, H. Nagao, W. Mori, M. Kamachi, and K. Yamaguchi, *Mol. Cryst. Liq. Cryst.*, **272**, 117 (1995).

41 T. Kawamoto and N. Suzuki, *J. Phys. Soc. Jpn.*, **63**, 3158 (1994).

42 V. Laget, S. Rouba, P. Rabu, C. Hornick, and M. Drillon, *J. Magn. Magn. Mater.*, **154**, L7 (1996).